Analysis of body-fin cooperative propulsion mechanism of koi carp using Pose Estimation⋆

Xin Wu[a], Yonghui Wang[c] and Lianming Wang[b,*]

[a]School of Physics, Northeast Normal University, Chang Chun, 130024, China
[b]School of Marine Information Engineering, Hainan Tropical Ocean University, San Ya, 572022, China
[c]Department of Computer Science, Prairie View A&M University, Prairie View, 77446, TX, USA

ARTICLE INFO

Keywords:
Fish
Body-fin Cooperative Propulsion
Pose and Motion Estimation Platform

ABSTRACT

The advancement of science and technology has led to the development of advanced underwater robots, significantly improving human beings' ability to explore, understand, and preserve the oceans. The study of fish movement holds crucial scientific and practical significance in advancing underwater robotics technology. It can reveal the secret behind the efficient swimming of fish and provide a basis for developing new underwater robots with low noise, high efficiency, high stability, and high mobility. This research establishes a fish body-fin synergistic propulsion model to analyze the synergistic propulsion mechanism of fish bodies and fins. A fish pose and motion estimation platform is constructed to provide data support for the analysis. The platform quantifies a koi's movement to analyze the fish wave characteristics for different swimming states. The proposed body-fin coordination model explores four koi swimming states (advancing, retreating, turning, and floating up), providing an innovative idea for fish movement research. The research results can significantly help the designing, developing, and optimizing modern underwater robots. The code and dataset for this research are available in https://github.com/wux024/AdamPosePlug.

1. Introduction

The scarcity of resources is an increasingly pressing concern in light of the rapid progress of science and technology, prompting humans to shift their focus toward the oceans. However, the complex marine environment presents a significant challenge for human movement underwater. Underwater robots, on the other hand, can operate freely in such harsh conditions and are therefore essential in various industries, such as the marine oil and gas, defense, maritime search and rescue, oceanographic research, underwater archaeology, and environmental monitoring sectors (Bogue, 2015).

Currently, electric propellers are the typical means of propulsion for underwater robots. However, multiple propellers are generally required to ensure freedom of movement, rendering these robots with complex shapes and structures and resulting in poor hydrodynamic and slewing performance.

Fish, having evolved over millions of years, have developed highly efficient locomotion skills, far exceeding those of traditional engineered marine locomotion systems. Their remarkable mobility and coordination make them a valuable source of inspiration for engineers to design and control new underwater robots within the framework of bionics. These robots, developed based on the principles of fish and other aquatic life, will become powerful tools to assist humans in exploring, monitoring, utilizing, and preserving the oceans (Bandyopadhyay, 2005; Vincent, 2006; Yu et al., 2018).

How fish move is a fundamental question in developing new underwater robots. The answer to this question holds significant scientific and practical value. On the one hand, understanding the biomechanical effects of fish swimming aids in comprehending fish behavior, physiology, and ecology. On the other hand, the mobility of fish provides the basis for research theory, which is significant in designing and controlling new underwater robots.

In recent years, computer vision-based recognition, detection, and measurement technologies have continuously developed. With the help of such technology and a certain number of cameras, features of a target object can be extracted and utilized. Some studies on fish movement analysis using computer vision methods have already been proposed. Some studies on fish movement analysis using computer vision methods have already been proposed.

In earlier research, Jing et al. (2004) used video to record fish movements and studied the kinematics of turning maneuvers of startled Crucian Carp (Carassius auratus) but was limited to observations in a two-dimensional plane. Li et al. (2005) studied the dorsal fin of Cymnarchus niloticus based on the predecessors and recorded more abundant motion parameters but remained confined to the two-dimensional plane observation. Yan et al. (2008) designed an earlier observation system to track the two-dimensional movement of fish. Wu (2010) proposed a video tracking system for measuring the 3D kinematics of free-swimming fish. Zhang et al. (2011) used X-ray photography technology to determine the number and length of vertebral body joints, which supported

⋆This research was partially sponsored by the *Major Science and Technology Projects in Sanya* (ZDKJ-SY-2020-001), the *Scientific Research Foundation of Hainan Tropical Ocean University* (No. RHDRC202001), and the *Major Science and Technology Projects of Hainan Province* (ZDKJ202017-02-01).

*Corresponding author: Lianming Wang
wux024@nenu.edu.cn (X. Wu); yowang@pvamu.edu (Y. Wang); lmwang@hntou.end.cn (L. Wang)
ORCID(s): 0000-0002-6250-4218 (X. Wu); 0000-0003-4334-0921 (Y. Wang); 0000-0002-3695-3909 (L. Wang)

the joint control of the carp-like bionic robot. Wang et al. (2013) introduced a high-speed camera system to analyze the 3D movements of koi. Voesenek et al. (2016) proposed a method to track fish swimming in 3D using multiple high-speed camera video systems. Mao et al. (2016) discussed the basic technology of occlusion tracking, studied the matching model of actual and imaginary fish occlusion, and realized 3D fish target non-occlusion tracking. Saberioon and Cisar (2016) developed multiple fish tracking systems based on currently available structured light sensors. Qian and Chen (2017) established a simple and economical device to detect the 3D motion of zebrafish, enabling scientists to track the 3D motion of multiple zebrafish at a low cost and with precise spatial location. Cheng et al. (2018) proposed a method for obtaining quantitative 3D trajectories of individuals in fish schools using synchronized cameras. A master-slave paradigm tracks fish in the master view with a convolutional neural network, then associates each fish with detections in the slave view by formulating cross-view data association as moment-wise linear assignment problems. Liu et al. (2019) proposed a method for 3-D tracking of fish groups using skeleton analysis. Feature points are simplified and associated with obtaining top-view trajectories, which are then matched with side-view feature points to obtain 3-D trajectories. Epipolar and motion continuity constraints are used in the matching process.

The analysis of fish movement has traditionally focused on 2D/3D motion tracking and simple motion pattern analysis. However, these analytical methods cannot analyze fish movement postures, such as how the caudal or pectoral fins work together during movements due to the disordered motion of animals or animal limbs. Consequently, extracting such motion features using traditional image processing methods is challenging and must be more comprehensive to analyze local complex motions. Therefore, a more efficient tool to extract more information (features or patterns) for analyzing local complex motions is needed, and such a method can extract more features and be applied to more scenes to solve the problems mentioned above.

Recently, the rapid development of deep learning-based computer vision technology has made it an efficient way of solving complex feature extraction problems.(Lauer et al., 2022) Deep learning models can quickly obtain the position and attitude of the target object in the target coordinate system. In computer vision, pose estimation is defined as identifying specific objects in an image and determining the position and orientation of each object relative to a particular coordinate system. Hence, applying pose estimation to the quantification of fish motion can solve the problems existing in current research. Fish movement is complex and unpredictable, and it is not easy to establish a hydrodynamic model that can fully describe it. Moreover, extracting motion features based on traditional computer vision techniques is complex, and more than the extracted features are needed to analyze local areas. Complex motion problems need to be urgently solved in fish motion analysis research.

This study aims to address the challenges in fish motion analysis by employing pose estimation based on modern computer vision technology. The quantitative analysis provides data support for analyzing the synergistic propulsion mechanism of fish bodies and fins. In particular, this paper proposes a model that can describe the synergistic propulsion of fish bodies and fins as comprehensively as possible to provide a theoretical basis for fish motion analysis. Our main contributions include the construction of a fish pose and motion estimation platform, studying fish body waves, and establishing a discrete model of fish body-fin synergistic propulsion.

The fish movement research platform constructed in this study provides a new method for fish movement research, and the research results of koi movement have specific reference significance for underwater robotics research. The proposed model and methodology have the potential for further applications in the analysis of complex motions in fish motion research and other fields. This study provides a valuable contribution to the development of computer vision technology in analyzing complex motions and establishing a theoretical basis for fish motion analysis.

2. Materials and methods

2.1. Fish and experimental setups

The experiments were performed using a koi carp, a subcarangiform swimmer. The carp (body length $L = 300$ mm) was housed in a water tank in the laboratory. The fish pose, and motion estimation platform is illustrated in Fig.1.A was constructed with high frame rate cameras plus the pose estimation-based motion parameter measurement algorithm (Wu et al., 2022). The platform consists of the following equipment: a water tank (120 cm × 20 cm × 30 cm in length, width, and depth, respectively), a high-performance computer, three high-frame-rate (210 FPS), and high-resolution (1280 × 1024 pixels) CCD cameras, a wave maker, and two fill lights (maximum power 100 W). Example images captured by the three cameras are shown in Fig.1.B. All videos recorded by the three cameras were synchronized by our proposed algorithm and then sent to the computer and stored in the computer's hard drive.

To analyze the koi motion, as shown in Fig.1.C, twenty-one key motion points are selected for labeling on the carp based on our estimation results: one on its head, one on each eye, four on its back, four on each pectoral fin, one on each side of the body, and four on the caudal fin. For detailed software and data of this study, please refer to`https://github.com/wux024/AdamPosePlug`. Moreover, please refer to `https://github.com/wux024/AdamPose` for more dynamic display results and detailed software information (Wu et al., 2022).

Once the koi's original motion data is obtained, the koi's motion and pose parameters (displacement, velocity, pose angle, and vibration frequency) are extracted using the motion parameter measurement method (Wu et al., 2022)

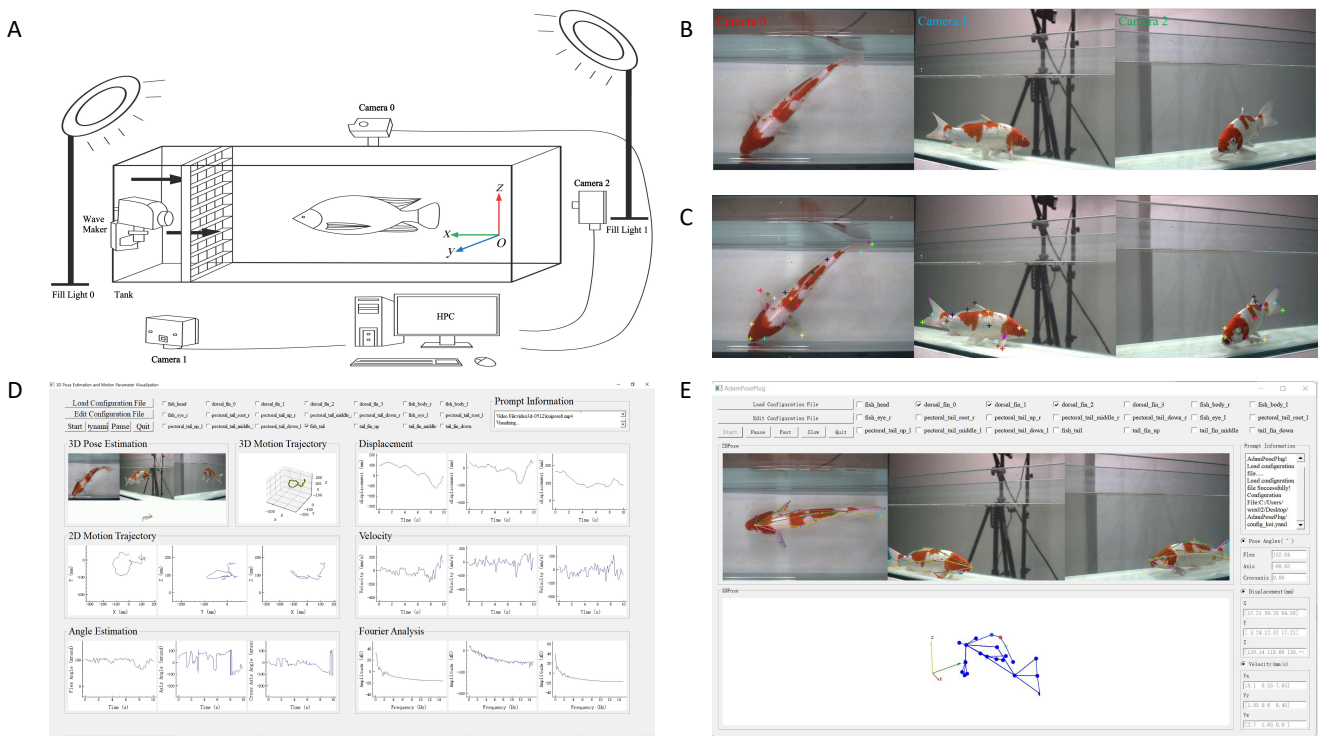

Figure 1: (A) Schematic diagram of fish pose and motion estimation platform; (B) Examples of captured images; (C) An example diagram of key points labeling of the koi; (D)(E) The graphical interface for fish movement data processing and visualization: the main window and the plug-in window.

based on pose estimation. These parameters can then be used to analyze the motion of the koi.

The graphical interface for pose estimation and motion parameter visualization, as shown in Fig.1.D and Fig.1.E, is designed to facilitate data processing and motion visualization. The graphical interface is divided into primary and plug-in windows. The main window mainly visualizes changing motion parameters with time, and the plug-in window mainly visualizes the selected key points, postures, and motion parameters. The interface runs stably and can independently select multiple key points for visualization.

The fish pose and motion estimation platform integrates data collection, processing, and analysis. The input is a video of fish moving in the tank from multiple perspectives. At the same time, the outputs are 2D and 3D pose estimations and motion parameters (2D/3D motion trajectory, displacement, velocity, acceleration, pose angle, and Fourier transformation). This platform provides solid data support for fish motion analysis. In this study, only movements of the koi in still water are studied, no flow and waves were created.

2.2. Fish wave model

Fish perform swimming by bending and swinging their bodies and fins. A diagram of fish body wave curve is shown in Fig.2. According to the observation results of fish in the BCF (Body and/or Caudal Fin) model (Webb, 1984), the expression of fish body wave $y(x,t)$ Lighthill (1960) obtained by fitting is:

$$y(x,t) = (c_0 + c_1 x + c_2 x^2)\sin(2\pi f t + kx) \tag{1}$$

where $y'(x) = c_0 + c_1 x + c_2 x^2$ is the envelope equation of the fish body wave, x represents the coordinate of any point on the fish body, c_0, c_1, and c_2 are envelope coefficients. The network coefficient, k, is the fish wave number and f is the caudal fin swing frequency.

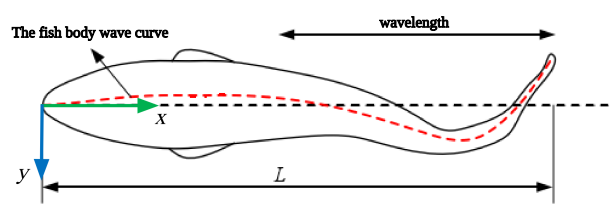

Figure 2: Schematic diagram of fish body wave curve.

More complete fish wave characteristics can be obtained if the fish body is modeled more accurately. For example, the fish body wave model established based on viscoelastic beam theory can be used to analyze fish swimming situation from the inside of the fish body (Valdivia y Alvarado, 2007; Nguyen et al., 2013), and its dynamic equation is a high-order partial differential equation. This type of model describes the complex modal characteristics of fish body waves. Its establishment involves relatively complex biomechanical principles, which is beyond the scope of this study. The main focus of this study is the experimental research method for analyzing biological motion. Without going into

details, an in-depth study of biomechanical principles can help design more accurate experiments.

2.3. A discrete model for fish body-fin synergistic propulsion

The water currents in the underwater environment where fish live are unstable, especially in the oceans. Due to the existence of waves, internal waves, currents, eddies, and other fluid phenomena, the water currents are not identical at different spatial locations and constantly change over time. In this complex water environment, fish rely on synergistic oscillations or fluctuations between their bodies and fins (pectoral, dorsal, caudal, ventral, and anal fins) to achieve free swimming, such as advancing, retreating, turning, floating up, sinking, and hovering. In this section, a discrete model is developed to qualitatively describe the synergistic propulsion of fish bodies and fins.

Firstly, the water flow environment where the fish is located can be defined as $\mathcal{E}$; and $\mathcal{M}$ ($m_i \in \mathcal{M}$) can be used to represent the fish swimming category set, where m_i may be advancing, retreating, turning, floating up, sinking, hovering, etc. Secondly, all observed parts form a target set which is defined as $\mathcal{F}$ ($f_j \in \mathcal{F}$), here f_j can be the caudal fin, left pectoral fin, right pectoral fin, left pelvic fin, right pelvic fin, anal fin, dorsal fin, etc. The fish body is defined as set $\mathcal{B}$. Finally, all possible states of the fish body parts, such as the fish body and each fin, are defined as a state set $\mathcal{P}$ ($p_k \in \mathcal{P}$), where p_k can be swung left, swing right, rapid swing, flapping up and down, paddling back and forth, clockwise rotation, counterclockwise rotation, left tilt, correct tilt, static, fin surface fluctuates downstream, fin surface fluctuates upstream, etc. The set elements can increase or decrease based on the actual observed results.

Therefore, a fish swimming event can be expressed as, in period T, under the water flow environment $\mathcal{E}$, the fish body $\mathcal{B}$ and each fin $\mathcal{F}$ being in certain state $\mathcal{P}$ work together to produce fish swimming $\mathcal{M}$. A state matrix $\mathcal{S}_t$ can be used to represent the state $\mathcal{P}_\mathcal{B}$ of the fish body $\mathcal{B}$ and the state of each fin, at the moment t. The rows of the matrix are determined by the target set $\mathcal{F}$, and the columns of the matrix are determined by the pose set $\mathcal{P}$, so the dimension of the matrix should be $\mathcal{F} \times \mathcal{P}$. An element s_{jk} of the matrix indicates whether fin f_j is in state p_k or not depending on whether $s_{jk} = 1$ or $s_{jk} = 0$. Thus, the swimming state of the fish in period T can be represented by

$$\mathcal{M} = \sum_{\mathcal{S}_t} \mathcal{E}(\mathcal{P}_\mathcal{B}, \mathcal{S}_t). \tag{2}$$

This formula shows that the swimming of a fish is a cumulative effect of various states produced by water current forced movements of the fish's body and each fin over a while. For example, a fish swimming forward in a straight line results from a relatively regular swing of the body or pectoral fins for a certain period.

Thus, by measuring the states of a fish in a time period t with relevant technologies, fish swimming can be characterized to a certain extent. For example, in a certain period of t, when the water flow environment is ε, the swimming state is m_i, and the fish body posture is $p^i_\mathcal{B}$, the state of each fin can be represented using state matrix $\mathcal{S}_t$, as shown in Table 1.

Table 1
State matrix $\mathcal{S}_t$

$\mathcal{E}$	$\mathcal{M}$	$\mathcal{P}_\mathcal{B}$	$\mathcal{F}$ \ $\mathcal{P}$	p_1	p_2	$\cdots$	p_k	$\cdots$
ε	m_i	$p^i_\mathcal{B}$	f_1	s_{11}	s_{12}	$\cdots$	s_{1k}	$\cdots$
			f_2	s_{21}	s_{22}	$\cdots$	s_{2k}	$\cdots$
			$\vdots$	$\vdots$	$\vdots$	$\ddots$	$\vdots$	$\vdots$
			f_j	s_{j1}	s_{j2}	$\cdots$	s_{jk}	$\cdots$
			$\vdots$	$\vdots$	$\vdots$	$\vdots$	$\vdots$	$\cdots$

Assuming there is a measurement system that can obtain $\mathcal{S}_t$ for any period t, when the fish body posture is $p^i_\mathcal{B}$, then after N measurements, the number of $s_{jk} = 1$ to N ratio represents the frequency of fin f_j being in state p_k. A more significant frequency will cause an effect m_i. Therefore, the qualitative description of the body-fin propulsion of fish swimming can be determined by using statistical laws. Combined with the continuous mathematical model, the mechanism of fish body-fin synergistic propulsion can be described more completely.

3. Results and discussions

The length of the koi in this research is about 30 cm. Combining with theoretical models and experimental data, the mechanism of synergistic propulsion of fish bodies and fins is analyzed from different perspectives. In this study, the experimental platform was used to simultaneously record 40-minute motion videos of the koi from three different angles. The videos were divided into 10-second segments for a total of 240 videos. The experiment is mainly divided into two parts:

(1) Using the fish body wave model to analyze the fish body wave characteristics in three koi swimming states (advancing, retreating, and turning); and

(2) Using the discrete model to analyze body-fin coordination of the koi in four different swimming states (advancing, retreating, turning, and floating up) and to determine the state tables of the koi in different swimming states and the motion parameters to maintain these states.

3.1. Fish wave analysis of the koi

This section mainly observes the fish body waves of the three swimming states of the koi: advancing, retreating, and turning. The fish body waves of these three motion states are the easiest ones to observe and relatively close to the ideal fish body waves.

Koi fish body wave analysis for advancing The advancing state of the koi over a time period is shown in Fig.3.A. The first row in the figure shows consecutive frames of the

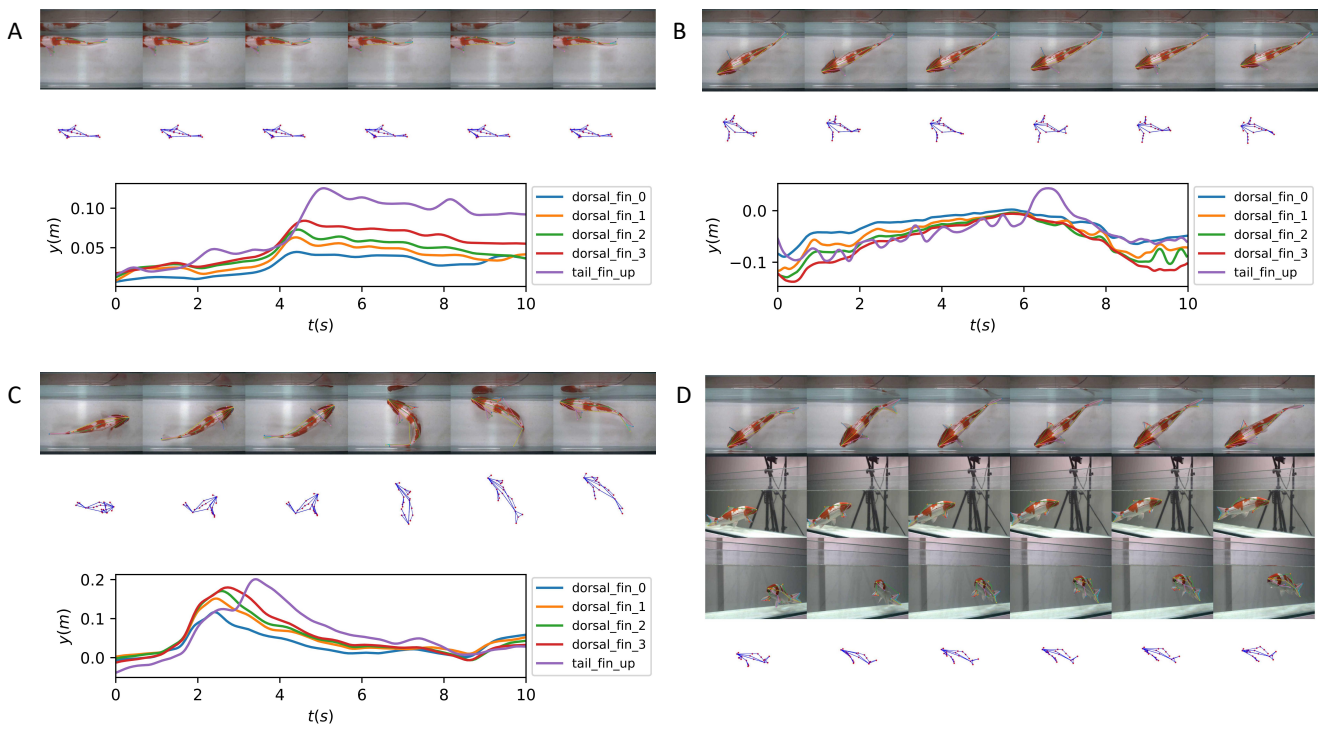

Figure 3: (A) Fish body wave analysis for the koi advancing state; (B) Fish body wave analysis for the koi retreating state; (C) Fish body wave analysis for the koi turning state; including consecutive frames showing fish poses and the 3D pose estimation from the virtual perspective; and the actual fish body wave curve of the koi advancing state. (D) An example of 3D pose estimation from different views and a virtual perspective when the koi floats up.

actual viewing angle, and the second row shows the 3D pose estimations from a virtual perspective. Both rows show slight bending of the fish's body. Pose estimation quantifies motion parameters for analyzing fish body waves as koi advances.

A total of 5 points, marked on the back of the fish at the locations of $x = 0.11, 0.15, 0.17, 0.21, 0.30\,\mathrm{m}$, are selected for the analysis. The y-direction displacements of these points are shown in Fig.3.A, plotted along the time axis.

According to equation (1), ideally, at any point of the fish body, the displacement in the y direction should be a sine wave, which is quite different from the actual measurement. The main reason is that the fish does not move periodically according to the ideal advancing direction. By comparing the curve with the actual swimming video, it is found that the fish body movement is in line with the actual situation.

Koi fish body wave analysis for retreating The actual motion of the koi's retreating state during a period and the 3D pose estimation of the virtual perspective are shown in Fig.3.B. The same key points of observation are used. The displacement curves of these points in the y direction along the time axis are shown in Fig.3.B. For retreating, the swing of the fish's body is not significant; instead, the body has a small amplitude quasi-periodic swing. The main driving parts for retreating are the left and right pectoral fins. Subsequent experiments will carry out a detailed analysis of this state.

Koi fish body wave analysis for turning The top view of the actual motion status of the koi turning state in a period and its 3D pose estimation are shown in Fig.3.C. The key points observed are the same as those in the previous two states. The displacements of the points in the y direction along the time axis are shown in Fig.3.C. For turning, the fish body first has a slow adjustment process, then swings wildly, and finally, after the turning is completed, the fish body swings and adjusts slightly. The primary body parts responsible for turning are the fish body and the caudal fin, while the other fins have little effect and do not provide significant driving forces. Subsequent experiments will give more detailed body-fin coordination.

3.2. Body-fin synergistic propulsion mechanism analysis

This section mainly measures the state transition matrix of four koi swimming states: advancing, retreating, turning, and floating up, and gives the motion parameters for each fin. The body-fin coordination process of sinking is similar to that of floating up, so no measurement for sinking is conducted. In addition, hovering is mainly adjusted by the fish body's internal buoyancy or small fluctuations, which is not within the scope of research on the body-fin synergistic propulsion mechanism.

In this study, the experimental conditions are: water flow environment $\mathcal{E}$ = **still water**; and swimming category set $\mathcal{M} = \{m_1$ (advancing), m_2 (retreating), m_3 (turning), m_4 (floating up), m_5 (sinking), m_6 (hovering)$\}$. The main fish

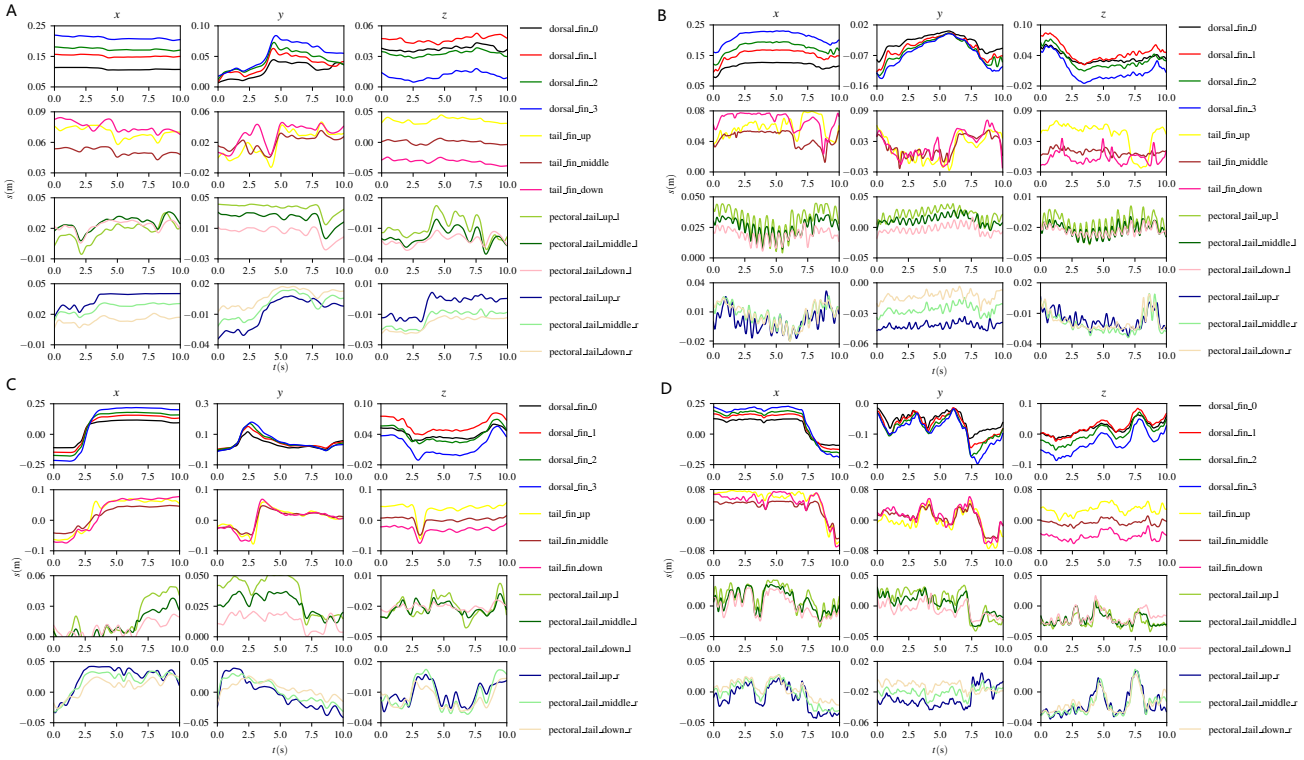

Figure 4: Relative displacement measurements of 13 key points as the koi moves (A) forward; (B) backward; (C) turns; and (D) floats up. The first row represents the change of the fish body; the second row represents the change of the caudal fin; the third row represents the change of the left pectoral fin; and the fourth row represents the change of the right pectoral fin.

Table 2
Koi advancing status table

$\mathcal{E}$	$\mathcal{M}$	$\mathcal{P}_{\mathcal{B}}$	$\mathcal{F}$ \ $\mathcal{P}$	p_1	p_2	p_3	p_4	p_5
still water	m_1	$p_2 + p_4/p_5$	f_1	0	1	0	1/0	1/0
			f_2	1/0	0	1/0	0	1/0
			f_3	1/0	0	1/0	0	1/0

body parts being observed are fish body $\mathcal{B}$ and fins $\mathcal{F} = \{f_1$ (caudal fin), f_2 (left pectoral fin), f_3 (right pectoral fin)$\}$. The movement state set for fins is defined as $\mathcal{P} = \{p_1$ (slap back and forth), p_2 (slap left and right), p_3 (slap up and down), p_4 (big flap), p_5 (small flap)$\}$.

Synergistic analysis of body and fins for koi advancing By analyzing the state of the fish advancing frame by frame in 240 videos, the state table tabulated in Table 2 exhibits the highest frequency. Thus Table 2 shows the state table S_t for koi advancing, where 1/0 indicates whether the state is present. Table 2 qualitatively describes the cooperation between the fish body and the three fins, which play significant roles when the koi moves forward. When the koi swims forward, the fish body swings left and right in a large or small movement ($p_2 + p_4/p_5$), and at the same time, the tail fin swings with the fish body in a large or small flap, which is the main driving force for the koi to move forward. In most cases, the left and right pectoral fins adjust the advancing posture through small back-and-forth strokes or up-and-down flaps, mainly to maintain the straightforward path and the position in the vertical direction. The following is a quantitative analysis of the body-fin coordination of the koi when it moves forward.

The plots of the movement parameters of the fish body's key points and each fin's key points (labeled as in Fig.1.C) when the koi moves forward can be used to analyze the body-fin coordination quantitatively. Fig.4.A shows the displacement curves of the four key points of the fish body relative to the fish head, the displacement curves of the three outer key points on the caudal fin relative to the base of the caudal fin, and the displacement curves of the outer key points on the left and right pectoral fins relative to the corresponding bases of the left and right pectoral fins. Each row shows the $s - t$ curves of different key points relative to the same body part in the three directions of x, y, and z. Fourier analysis of these curves approximates the flapping frequency.

From Fig.4.A, it can be seen that, when the koi swims forward, the fish body slowly swings in the y direction, and the maximum swing amplitude exceeds 7.5 cm. At the same time, the caudal fin either sways extensively in the y direction with the fish body or sways slightly not synchronized with the fish body. The maximum sway of the caudal fin exceeds 3 cm, and the frequency of its big swings is about 0.25 Hz, while the frequency of the small swings is about 1.67 Hz. The left and right pectoral fins flap slightly back and forth and up and down. The maximum amplitude of the back-and-forth flaps exceeds 2 cm, and the flapping frequency

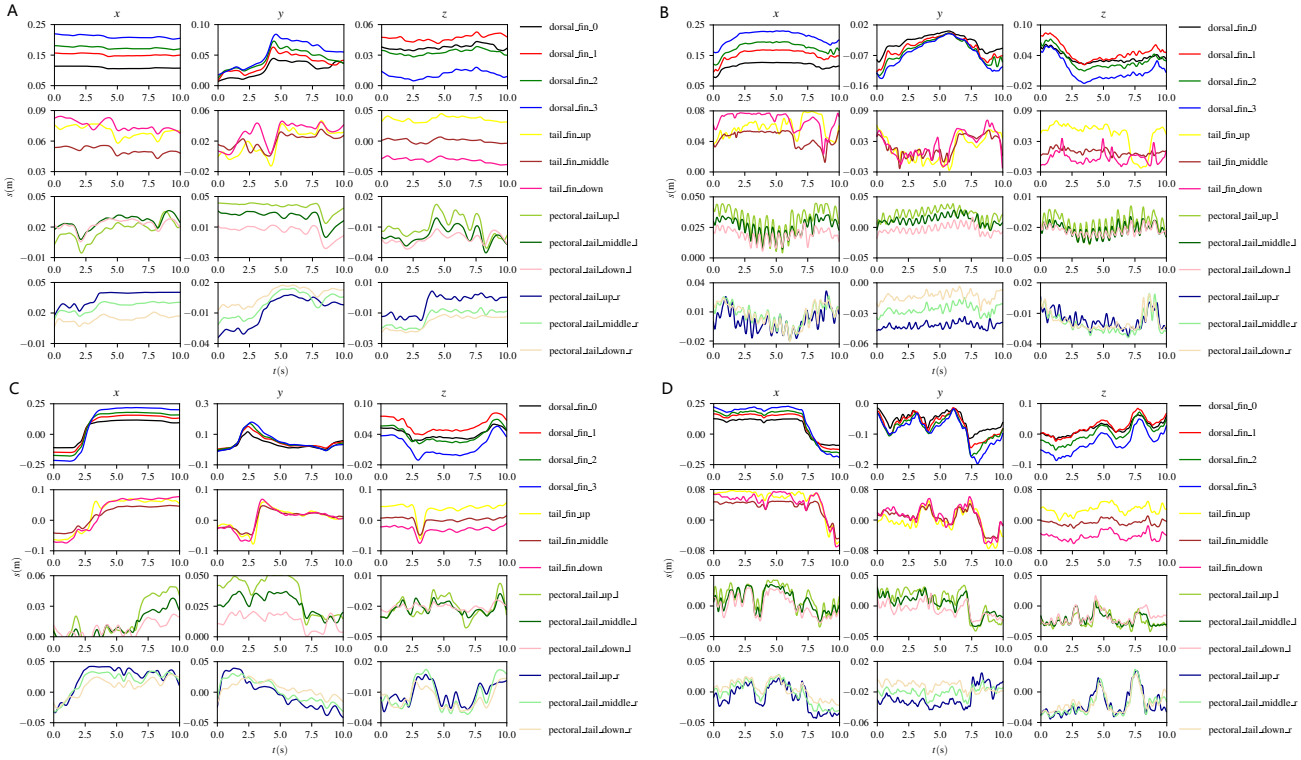

Figure 5: The deformation measurements of each fin when the koi moves (A) forward; (B) backward; (C) turns; and (D) floats up. The first row is the deformation of the caudal fin; and the second and third rows are the deformation of the left and right pectoral fins, respectively.

is about 0.167 Hz. The maximum amplitude of the up-and-down flaps exceeds 2 cm, and the flapping frequency is about 0.89 Hz.

In addition, when fish swims, each fin will deform, and the pose angle can be used to measure the bending degree of each fin. The visual result of the deformation measurement of each fin is shown in Fig.5.A. From Fig.5.A, it can be seen that the koi fins deform when the fish swims forward. According to the definition of attitude angle, the first column of the figure represents the flexion and extension angle, and the variation range of the caudal fin flexion and extension angle is $95.0° \sim 116.8°$. The variation range of the left pectoral fin flexion and extension angle is $123.0° \sim 140.4°$, and the range of the right pectoral fin flexion and extension angle is $103.9° \sim 158.1°$. The second and third columns of the figure represent complex rotations, which are directional and more complex deformations. These complex deformations are mainly to maintain the fish's balance and control its movement's direction.

Synergistic analysis of body and fins for koi retreating The fish body parts to be measured are the same as those for fish advancing. By analyzing the state of the fish retreating frame by frame in the 240 videos, the state table tabulated in Table 3 exhibits the highest frequency, thus Table 3 is the koi retreating state table S_t, where 1/0 in the table indicates whether the state is present or not. Table 3 qualitatively describes the coordination of the fish body, caudal fin, and pectoral fins when the koi moves backward. When the koi

Table 3
Koi retreat status table

$\mathcal{E}$	$\mathcal{M}$	$\mathcal{P}_B$	$\mathcal{F}$ \ $\mathcal{P}$	p_1	p_2	p_3	p_4	p_5
still water	m_2	hardly move	f_1	0	0	0	0	0
			f_2	1/0	0	1/0	0	1/0
			f_3	1/0	0	1/0	0	1/0

retreats, because it cannot look back, its body's displacement in the y direction is relatively large without swinging left and right. While the caudal fin moves little, the pectoral fins drive the koi's retreat. In most cases, the left and right pectoral fins adjust the retreat posture and provide the main drive through small back-and-forth strokes or up-and-down flaps. The fish's moving speed is slow when it retreats because the power provided by the pectoral fins is insufficient. A quantitative analysis of the body-fin coordination of the koi when it retreats is provided below.

It can be seen from Fig.4.B that when the koi swims backward, the caudal fin does not have apparent periodic movement but has a high deformation frequency. The left pectoral fin flaps back and forth with relatively high frequency. The maximum swing amplitude is about 2 cm, and the swing frequency is about 2 Hz. In addition, its up-and-down stroke amplitude exceeds 2 cm, and the stroke frequency is about 2.5 Hz. The right pectoral fin is not highly synchronized with the left pectoral fin. Its back-and-forth

Table 4
Koi turning status table

$\mathcal{E}$	$\mathcal{M}$	$\mathcal{P}_B$	$\mathcal{F}$ \ $\mathcal{P}$	p_1	p_2	p_3	p_4	p_5
still water	m_3	$p_1 + p_4$	f_1	1	0	0	1	0
			f_2	0	0	1/0	0	1/0
			f_3	0	0	1/0	0	1/0

Table 5
Koi floating up status table

$\mathcal{E}$	$\mathcal{M}$	$\mathcal{P}_B$	$\mathcal{F}$ \ $\mathcal{P}$	p_1	p_2	p_3	p_4	p_5
still water	m_4	$p_1 + p_5$	f_1	0	1	0	0	1
			f_2	1/0	0	1/0	0	1
			f_3	1/0	0	1/0	0	1

stroke frequency is high, the maximum swing amplitude is about 3 cm, and the swing frequency is about 1.32 Hz; while the up-and-down flap amplitude is about 2 cm and the flapping frequency is about 1.5 Hz. The asynchrony of the left and right pectoral fins is one of the main reasons for its tortuous moving path as the fish retreats.

It can be seen from Fig.5.B that, in retreating, the koi fins deform with relatively high deformation frequency. The first column of the figure shows that the range of flexion and extension angle of the caudal fin is 16.8° ∼ 126.9°; the range of flexion and extension angle of the left pectoral fin is 73.2° ∼ 165.3°; and the range of flexion and extension angle of the right pectoral fin is 70.5° ∼ 149.3°. The second and third columns of the figure represent complex rotations, which are directional and more complex deformations. These complex deformations are mainly to maintain the balance of the fish and control the direction of its retreat.

Synergistic analysis of body and fins for koi turning The same fish body parts used to analyze fish advancing are used. Through the frame-by-frame analysis of the fish body turning videos, the status table, as tabulated in Table 4, has the highest frequency. Thus the state table S_t for koi turning is shown in Table 4. Here 1/0 in the table indicates whether the state is present or not. Table 4 qualitatively describes the coordination between the fish body, caudal fin, and pectoral fins when the koi turns. When the koi turns, the fish body bends considerably, and the tail fin also bends significantly with the fish body with a relatively high frequency. The pectoral fins do not play significant roles in the turning process, and their small up-and-down flaps are mainly to maintain the fish's posture. The following is a quantitative analysis of the body-fin coordination for koi turning.

When the koi turns to the left, the fish body bends considerably (p_1+p_4). As can be seen from Fig.4.C, together with the fish body, the tail fin bends considerably with a high frequency. The entire turning process is completed in about 4 s, and the swing range of the tail fin is about 12 cm. During this left-turning process, the right pectoral fin is retracted to its belly, and the left pectoral fin is kept away from the belly to maintain the balance of the fish body through deformations. The turning process depends on the body's sudden movement, while the fins mainly balance and control the turning direction.

Fig.5.C reflects the deformations of the koi fins in the turning process. The figure's first column shows that the variation range of caudal fin flexion and extension angle is 102.2° ∼ 127.1°, the variation range of left pectoral fin flexion and extension angle is 94.6° ∼ 164.6°, and the variation range of right pectoral fin flexion and extension angle is 53.7° ∼ 152.0°. The second and third columns of the figure represent complex rotations, which are directional and more complex deformations. These complex deformations mainly maintain the fish's balance and control its turning direction.

Synergistic analysis of body and fins for koi floating up Fig.4.D shows consecutive frames from a video of the koi floating up. The first three rows are consecutive frames of the actual observation perspectives and the last row is the 3D pose estimation under the virtual perspective.

By analyzing the state of the fish floating up frame by frame in the 240 videos, the frequency of the state table tabulated in Table 5 is the highest. Therefore, the koi floating up state table S_t is shown in Table 5, where 1/0 in the table indicates whether the state is present or not. Table 5 qualitatively describes the coordination of the fish body, tail fin, and pectoral fins when the koi floats up. When the koi floats up, the fish body swings slightly from side to side ($p_1 + p_5$), while the tail fin follows the fish body and swings with small amplitudes but relatively high frequency. With slight flapping, the pectoral fins play an essential role in the floating up process, and they help the fish maintain its posture and provide a particular driving force. The following quantitatively analyses the body-fin coordination for koi floating up.

It can be seen from Fig.4.D that, when the koi floats up, the fish body swings left and right with large amplitude, the maximum swing amplitude is about 8 cm, and the swing frequency is about 0.4 Hz. The caudal fin moves with the fish body at a small amplitude, the maximum amplitude of the movement is about 5 cm, and the movement frequency is about 0.4 Hz. The swing amplitudes of the pectoral fins are negligible. Their maximum swing amplitude is about 2 cm, the swing frequency of the left pectoral fin is about 1.5 Hz, while the swing frequency of the right pectoral fin is 1.2 Hz.

Fig.5.D reflects the koi fin deformations in the floating-up process. As shown in the first column, the variation range of caudal fin flexion and extension angle is 87.9° ∼ 133.1°, the variation range of left pectoral fin flexion and extension angle is 51.6° ∼ 167.0°, and the variation range of right pectoral fin flexion and extension angle is 58.1° ∼ 157.4°. The flexion and extension angle variations of the fins for floating up are far more severe than those for the previous three motion states. The second and third columns of the figure represent complex rotations, which are directional and more complex deformations. These complex deformations

are mainly to maintain the balance of the fish and control its direction of floating up.

This section analyzes the quantitative results of the fish attitude and motion estimation platform, combined with the established fish body-fin synergistic propulsion discrete model, the body-fin synergistic propulsion mechanisms of the four koi swimming states in still water. The body-fin synergistic propulsion mechanism provides qualitative and quantitative descriptions of koi swimming. It demonstrates the validity of the proposed motion estimation-based method for analyzing fish body-fin synergistic propulsion mechanism. For a koi with body length L swimming in still water, the body-fin coordination mechanisms in four swimming states (advancing, retreating, turning, and floating up) are summarized as follows.

(1) When the koi moves forward, the fish body swings left and right with amplitude $A_1 < 0.34L$, and the swing frequency is 0.28 Hz< f_1 <0.67 Hz. At the same time, the tail fin swings together with the fish body at an amplitude of $A_2 \approx A_1$, and a swing frequency at $f_2 \approx f_1$; or it does not swing together with the fish body with an amplitude of $A_3 < 0.17L$, and a swing frequency at $f_3 = 3.0 \sim 7.0f_1$. The left and right pectoral fins move back and forth or flap up and down, and the flap frequencies are $f_4 = 0.5 \sim 1.0f_1$ and $f_5 = 0.5 \sim 1.0f_3$.

(2) To retreat, the koi mainly depends on the back-and-forth and up-and-down strokes of the left and right pectoral fins, while the fish body and tail fin provide a low contribution. The left pectoral fin's back-and-forth stroke frequency is 2 Hz< f_6 <3 Hz, yet the right pectoral fin is not highly synchronized with the left pectoral fin, and its back-and-forth stroke frequency is 2 Hz< f_7 <3 Hz, where $f_6 \neq f_7$. The asynchrony of the left and right pectoral fins is one of the main reasons for the koi's tortuous retreating path.

(3) When the koi turns left (right), it is mainly done by rapid fish body and tail fin movements. The fish body significantly bends, with a bending amplitude upper limit of $0.6L$. Together with the body, the caudal fin significantly bends with the bending amplitude upper limit of $0.4L$. At the same time, the right (left) pectoral fin is retracted to the fish belly, while the left (right) pectoral fin is kept away from the fish belly.

(4) When the koi floats up, the fish body swings left and right with the amplitude $A_4 < 0.27L$ and the swing frequency f_8 <0.5 Hz. At the same time, the caudal fin swings left and right with the amplitude $A_5 < 0.17L$ and the swing frequency f_9 <0.5 Hz, where $f_8 \approx f_9$. The left and right pectoral fins flap up and down, while the flapping frequency of the left pectoral fin is f_{10} <2 Hz and the flapping frequency of the right pectoral fin is f_{11} <2 Hz, where $f_{10} \neq f_{11}$.

During all these processes, each fin undergoes complex deformation, and the deformation includes complex fin surface fluctuations. These complex deformations are mainly to maintain the balance of the fish body and control the moving directions.

3.3. Discussion

This section presents a comprehensive analysis of the fish body wave characteristics of the three koi swimming states in conjunction with the fish body wave model. The findings reveal that the measured fish body waves differ substantially from the theory for two primary reasons. Firstly, in actual observation, despite setting several conditions to restrict the movement of the fish, the fish tend to deviate from the planned route. Nonetheless, the measured fish wave curve is still consistent with the koi swimming rule, and the fish wave changes can be observed from the curves. Secondly, the model must be more complex to describe the fish wave characteristics entirely. From the fish body wave model established based on the viscoelastic beam theory mentioned before, it is evident that the complexity of a simplified fish body wave model is already very high. Therefore, much research must be carried out to study fish body wave models.

This section also delves into the fish movement study using the proposed discrete model. The discrete model of fish body-fin synergistic propulsion primarily focuses on the qualitative description of the fish body-fin synergistic propulsion mechanism, which has significant reference value in the research on the control method of underwater robots. However, the model has many limitations since it cannot reveal the fish's movement mechanism from the inside. Thus, from an experimental perspective, further essential features may be discovered through the fusion of various types of sensor data for the study of fish movement. Although multi-source sensor data fusion is complex, the existing multi-modal learning technology provides a significant idea for solving this problem. For example, combining information from two modalities of infrared thermal imaging and pose estimation may help quantify fish movement more accurately and comprehensively. Therefore, the fusion of sensor data is a promising study area for enhancing our understanding of fish movement and improving the accuracy of existing fish body wave models.

4. Conclusion

This study presents a comprehensive analysis of fish motion and the associated propulsion mechanism by constructing a fish pose and motion parameter estimation platform. The platform comprises raw data collection of fish movement and quantification algorithms. A discrete model is established to qualitatively describe fish body-fin propulsion, providing a solid theoretical basis for analyzing the synergistic propulsion mechanism of fish bodies and fins. The koi body-fin synergistic propulsion mechanism is used as an example to analyze the fish body wave characteristics in three swimming states (advancing, retreating, and turning), and the state matrices of the koi are determined. These

matrices show the relationships between swimming states (advancing, retreating, turning, and floating up) and the motion parameters corresponding to the fish body and each fin. The experiments obtain a simple body-fin coordination mechanism corresponding to the four koi swimming states.

The platform constructed in this study provides new insights into fish movement research and has significant implications for designing, developing, and optimizing new underwater robots. Future research can extend the experiments to flowing water and other complex environments for more accurate results. Fusing various types of sensor data and related technologies based on multi-source information fusion can also promote neurobiological research. Multimodal learning techniques, such as combining information from particle images, infrared thermal imaging, and pose estimation, may help quantify fish movement and uncover the nature of fish swimming from the inside out. Overall, this study contributes to advancing fish motion research and has broad applications in underwater robotics.

CRediT authorship contribution statement

Xin Wu: Conceptualization, Methodology, Software, Validation, Formal Analysis, Investigation, Data Curation, Writing – Original Draft Preparation, Visualization. **Yonghui Wang:** Writing – Review & Editing, Supervision. **Lianming Wang:** Investigation, Resources, Writing – Review & Editing, Supervision, Project Administration, Funding Acquisition.

References

Valdivia y Alvarado, P.P.A., 2007. Design of biomimetic compliant devices for locomotion in liquid environments. Ph.D. thesis. Massachusetts Institute of Technology. Massachusetts.

Bandyopadhyay, P.R., 2005. Trends in biorobotic autonomous undersea vehicles. IEEE Journal of Oceanic Engineering 30, 109–139. doi:10.1109/JOE.2005.843748.

Bogue, R., 2015. Underwater robots: a review of technologies and applications. Industrial Robot: An International Journal 42, 186–191. URL: https://doi.org/10.1108/IR-01-2015-0010, doi:10.1108/IR-01-2015-0010.

Cheng, X.E., Du, S.S., Li, H.Y., Hu, J.F., Chen, M.L., 2018. Obtaining three-dimensional trajectory of multiple fish in water tank via video tracking. Multimedia Tools and Applications 77, 24499–24519. URL: https://doi.org/10.1007/s11042-018-5755-5, doi:10.1007/s11042-018-5755-5.

Jing, J., Yin, X., Lu, X., 2004. Hydrodynamic analysis of c-start in crucian carp. Journal of Bionic Engineering 1, 102–107. URL: https://doi.org/10.1007/BF03399460, doi:10.1007/BF03399460.

Lauer, J., Zhou, M., Ye, S., Menegas, W., Schneider, S., Nath, T., Rahman, M.M., Santo, V.D., Soberanes, D., Feng, G., Murthy, V.N., Lauder, G., Dulac, C., Mathis, M.W., Mathis, A., 2022. Multi-animal pose estimation, identification and tracking with deeplabcut. Nature Methods 19, 496–504. URL: https://doi.org/10.1038/s41592-022-01443-0, doi:10.1038/s41592-022-01443-0.

Li, F., jiang Hu, T., ming Wang, G., cheng Shen, L., 2005. Locomotion of gymnarchus niloticus : Experiment and kinematics. Journal of Bionic Engineering 2, 115–121. URL: https://doi.org/10.1007/BF03399488, doi:10.1007/BF03399488.

Lighthill, M.J., 1960. Note on the swimming of slender fish. Journal of Fluid Mechanics 9, 305–317. URL: https://www.cambridge.org/core/article/note-on-the-swimming-of-slender-fish/1DB2368914AD61BD29F5849AA5C5C236, doi:DOI:10.1017/S0022112060001110.

Liu, X., Yue, Y., Shi, M., Qian, Z.M., 2019. 3-d video tracking of multiple fish in a water tank. IEEE Access 7, 145049–145059. doi:10.1109/ACCESS.2019.2945606.

Mao, J., Xiao, G., Sheng, W., Qu, Z., Liu, Y., 2016. Research on realizing the 3d occlusion tracking location method of fish's school target. Neurocomputing 214, 61–79. URL: https://www.sciencedirect.com/science/article/pii/S0925231216305215, doi:https://doi.org/10.1016/j.neucom.2016.05.067.

Nguyen, P.L., Do, V.P., Lee, B.R., 2013. Dynamic modeling of a non-uniform flexible tail for a robotic fish. Journal of Bionic Engineering 10, 201–209. URL: https://www.sciencedirect.com/science/article/pii/S1672652913602164, doi:https://doi.org/10.1016/S1672-6529(13)60216-4.

Qian, Z.M., Chen, Y.Q., 2017. Feature point based 3d tracking of multiple fish from multi-view images. PLOS ONE 12, e0180254–. URL: https://doi.org/10.1371/journal.pone.0180254.

Saberioon, M.M., Cisar, P., 2016. Automated multiple fish tracking in three-dimension using a structured light sensor. Computers and Electronics in Agriculture 121, 215–221. URL: https://www.sciencedirect.com/science/article/pii/S0168169915003968, doi:https://doi.org/10.1016/j.compag.2015.12.014.

Vincent, J.F.V., 2006. Applications — influence of biology on engineering. Journal of Bionic Engineering 3, 161–177. URL: https://doi.org/10.1016/S1672-6529(06)60020-6, doi:10.1016/S1672-6529(06)60020-6.

Voesenek, C.J., Pieters, R.P.M., van Leeuwen, J.L., 2016. Automated reconstruction of three-dimensional fish motion, forces, and torques. PLOS ONE 11, e0146682–. URL: https://doi.org/10.1371/journal.pone.0146682.

Wang, L., Xu, M., Liu, B., Low, K.H., Yang, J., Zhang, S., 2013. A three-dimensional kinematics analysis of a koi carp pectoral fin by digital image processing. Journal of Bionic Engineering 10, 210–221. URL: https://www.sciencedirect.com/science/article/pii/S1672652913602176, doi:https://doi.org/10.1016/S1672-6529(13)60217-6.

Webb, P.W., 1984. Form and function in fish swimming. Scientific American 251, 72–83. URL: http://www.jstor.org/stable/24969414.

Wu, G., 2010. Measuring the three-dimensional kinematics of a free-swimming koi carp by video tracking method. Journal of Bionic Engineering 7, 49–55. URL: https://www.sciencedirect.com/science/article/pii/S1672652909601906, doi:https://doi.org/10.1016/S1672-6529(09)60190-6.

Wu, X., Wang, Y., Chen, L., Zhang, L., Wang, L., 2022. Motion parameters measurement of user-defined key points using 3d pose estimation. Engineering Applications of Artificial Intelligence 110, 104667. URL: https://linkinghub.elsevier.com/retrieve/pii/S0952197622000045, doi:10.1016/j.engappai.2022.104667.

Yan, H., min Su, Y., Yang, L., 2008. Experimentation of fish swimming based on tracking locomotion locus. Journal of Bionic Engineering 5, 258–263. URL: https://doi.org/10.1016/S1672-6529(08)60033-5, doi:10.1016/S1672-6529(08)60033-5.

Yu, J., Wang, M., Dong, H., Zhang, Y., Wu, Z., 2018. Motion control and motion coordination of bionic robotic fish: A review. Journal of Bionic Engineering 15, 579–598. URL: https://doi.org/10.1007/s42235-018-0048-2, doi:10.1007/s42235-018-0048-2.

Zhang, Y., He, J., Zhang, G., 2011. Measurement on morphology and kinematics of crucian vertebral joints. Journal of Bionic Engineering 8, 10–17. URL: https://www.sciencedirect.com/science/article/pii/S1672652911600061, doi:https://doi.org/10.1016/S1672-6529(11)60006-1.